

# A Study on Metastable Pitting of Alloy 690 in Chloride Solutions at 90°C

Zhi Jun Bai and Hyuk Sang Kwon

*Department of Materials Science and Engineering, Korea Advanced Institute of Science and Technology  
Taejon 305-701, South Korea*

Metastable pitting behavior of alloy 690 in chloride solutions at 90°C was explored using potentiodynamic and potentiostatic polarization methods. The results indicated that there existed a critical concentration of chloride ion of 0.01M above which alloy 690 is susceptible to pitting corrosion. Susceptibility of the alloy to metastable pitting increases with applied potentials at 0.01 M Cl<sup>-</sup> concentration and increasing the Cl<sup>-</sup> concentration at a fixed applied potential of 0 mV. The metastable pitting events were characterized by a slow increase in the anodic current followed by a quick drop. The repassivation time had some dependence on Cl<sup>-</sup> concentration and applied potential and all lied between 1 to 2 s. Corrosion types occurred during metastable pitting can be distinguished by the roll-off slope in the power spectral density plot ; 0 represent film dissolution, -1 represented metastable pitting and -2.5 represented pitting corrosion.

**Keywords** : metastable pitting, alloy 690, chloride solution, power spectral density

## 1. Introduction

Nickel based alloy 600 and alloy 690 were used widely in nuclear industry as steam generator (SG) tubing materials. Since alloy 690, with main composition Ni-30Cr-10Fe (wt. %), has higher resistance to corrosion than alloy 600 because of its high Cr content, alloy 600 tubes have been replaced with alloy 690 tubes for pressurized water reactors (PWRs) recently. But the corrosion of this alloy continues to be a serious problem, particularly pitting and pitting induced stress corrosion cracking (SCC) has become the principal failure mode leading to tube plugging in the worldwide.<sup>1)</sup>

In general, potentiodynamic anodic polarization was applied widely in the study of electrochemical behaviors for Ni based alloys<sup>2-6)</sup> to get some information such as pitting potential and corrosion potential. Recently, it is well recognized that the breakdown of passive film and its repair may occur at potentials below the potential required for stable pitting on some stainless steels,<sup>7-10)</sup> aluminum and its alloys<sup>11-13)</sup> et al.) or carbon steel,<sup>14-16)</sup> viz. metastable pitting.

The stages of pitting include passive film breakdown, metastable pitting (initiation, propagation and repassivation) and pit growth, and the metastable pitting stage was thought to be the most important since only pits that survive this stage could become stable growing pits.<sup>17)</sup> So,

a better understanding of pit initiation, stabilization, and growth may be gained from a thorough investigation of metastable pitting.<sup>17)</sup>

Many investigations have been performed to study the metastable pitting behavior of stainless steel, aluminum alloys or some pure metal such as iron, aluminum, and carbon steel. Few works were investigated on Ni based steels. Chloride anion, as the major contaminants, may be present in pressurized water reactor (PWR) and affect the material performance. Although the bulk concentration of contaminant may be only a few ppm, it is believed that the concentration of impurities in creviced regions can be increased to as high as four orders of magnitude.<sup>19)</sup> Chloride anion was thought as the most aggressive specie inducing pitting of nickel base alloys.<sup>4)</sup>

The objective of this research is to study the effects of Chloride concentrations and applied potential on metastable pitting, transition from metastable to stable pitting and mechanism of metastable pitting for alloy 690 in chloride solutions at 90°C.

## 2. Experimental

Commercial alloy 690 was used as working electrodes. The compositions (wt. %) of the testing alloy are as follows; Ni:59.2, Cr:30.4, Fe:9.5, and C:0.014. The alloy had been subjected to thermal treatment (solution anneal-

ling 1150°C, 30 min., followed by cold water quenching). The specimens were cutting to sheet of 15 × 15 × 2mm, and embedded in epoxy resin. The electrode surfaces were ground with emery paper to 1200 grit. The surfaces of the electrodes were sealed with silicon adhesive with an exposed area of about 1 cm<sup>2</sup> to the solution. The surfaces were cleaned by ultrasonic wave in high pure ethanol bath and rinsed in a distill water and dried by cool nitrogen prior to testing. A platinum counter electrode and a saturated calomel electrode with a salt bridge were used in tests (in this paper, all the electrode potential is referred to SCE). A conventional three-electrode electrochemical cell with volume of 1000ml was used.

Potentiodynamic and potentiostatic polarization tests were carried out with EG&G 273 potentiostat and M352 electrochemical software. The specimen first was cathodic cleaned by -1.0 V (SCE) for 300 s to remove air-formed film and then wait in stable OCP for 3600 s, finally starting test (The same pretreatments were use in all tests). Potentiodynamic polarization test start from the potential of 250mV below open circuit potential (OCP) to 1200 mV (free pitting solution) or the potential just above pitting potential. Potentiostatic tests were performed under the fixed potential from OCP for 3600s (or stop in the case that pitting took place). In all these tests, scan rate was 1 mV/s, and sampling frequency was 1Hz.

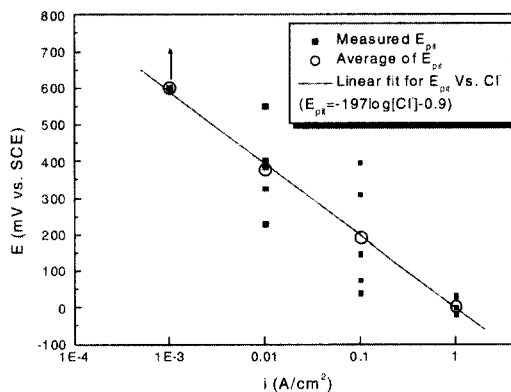
### 3. Results

#### 3.1 Polarization curves

The potentiodynamic polarization curves of alloy 690 in deaerated various Cl<sup>-</sup> concentrations at 90 °C are shown in Figure 1. In higher concentration of Cl<sup>-</sup> solutions (0.01, 0.1 and 1 M Cl), pitting potential can be get but not in dilute solutions (0.001 M and 0.0001 M Cl) where no

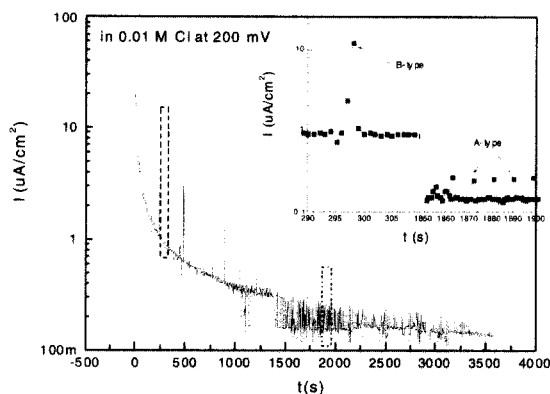
pitting corrosion took place. Comparing the figure 1 (a) and (b), we can found that the polarization curves of alloy 690 in dilute Cl<sup>-</sup> (0.001 M and 0.0001 M Cl) had the similar behavior with those in buffer solution and distill water. There was no pitting corrosion but transpassive dissolution around 400 mV in free chloride solutions that may correspond to the transpassive of Cr. On the other hand, alloy 690 was difficult to form stable passive film in distill water but formed stable film in buffer or Chloride solutions below the pitting potential or transpassive potential region. In the potential region of above 500 mV, alloy 690 can re-passived in buffer and 0.0001 M Cl solutions but not in dense Cl<sup>-</sup> solutions.

Figure 2 also showed that a distribution of pitting potentials existed at dense Cl<sup>-</sup> concentration (in 1M and 0.001 M Cl, 3 tests were carried out and 5 tests in 0.1 M and 0.01 M Cl<sup>-</sup> solutions). As mentioned above, in 0.001 M Cl solutions, no pitting can be found, the potential of 600 mV corresponded to lager current density can be explained



**Fig. 2.** Epit of alloy 690 as function of Cl<sup>-</sup> concentration in deaerated solutions at 90°C, data from the anodic polarization curves (at least 3 identical experiments at each concentration, in 0.001M Cl<sup>-</sup> and 0.0001 M Cl<sup>-</sup> solution, no pitting)

**Fig. 1.** potentiodynamic polarization curves for alloy 690 in deaerated various Cl<sup>-</sup> solutions, at 90°C, 1mV/s, (a)1M to 0.0001 M Cl<sup>-</sup> (b)0 M Cl<sup>-</sup> (distill water and buffer solution)



**Fig. 3.** Typical current transient of alloy 690 in deaerated 0.01 M NaCl solution at 90°C at 200 mV (SCE), sampling frequency: 1Hz. Also shown the typical single transient (me-tastable pitting), A-type: fast current rise and a fast fall, B-type: slow current rise followed a quick fall

by transpassive dissolution. In 0.1 M and 0.01 M Cl solutions, there existed a large scatter distribution of pitting potentials. Because no apparent crevice corrosion was found by after microscopic tests, so there may be a real statistical distribution of pitting potentials just found by other authors<sup>13,24)</sup> on other metals.

From these results, we can obtain a conclusion that there is a critical Cl<sup>-</sup> concentration to cause pitting corrosion for alloy 690 in Cl<sup>-</sup> solution that is 0.01 M Cl in given conditions.

### 3.2 Anodic current transients

Figure 3 showed a current transient of alloy 690 in 0.01 M Cl at 200 mV, which is the representative of current transients for alloy 690 in Cl<sup>-</sup> solution under potentiostatic conditions below pitting potential ( $E_{pit}$ ). It showed the background current density decayed with time. Superimposed on the background current, are many anodic current spikes can be distinguished from the background current fluctuations which lie above and below a current mean. The current density decreased with time within about the first 1000 s steeply then more gradually and during the experiment time did the anodic current show a permanent drop with time. In other words, the passive film became more stable with the given time during experimental conditions. The two typical kinds of current spikes were shown in insert of this Figure: the first type of transients (we called A-type) was characterized by a sharp increase in the anodic current followed by a quick drop. In general, this typed spike lasted a short time, in this sampling frequency (1Hz), raising time and dropping time all are 1 s and the heights for this transient is smaller than other type of transient. The second type of current transient displayed a type with a slow rise in current

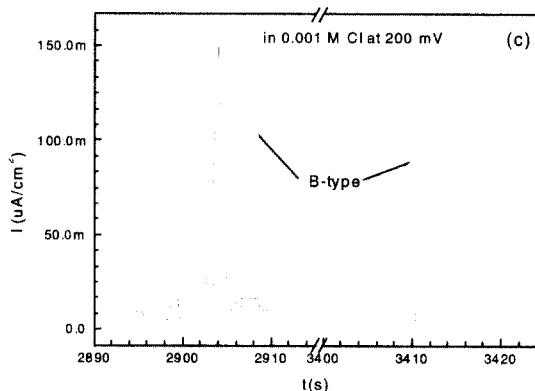
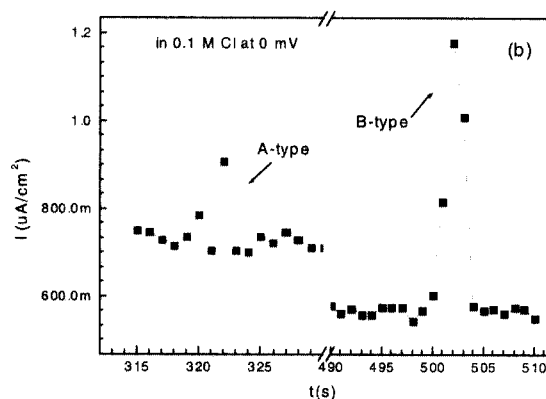
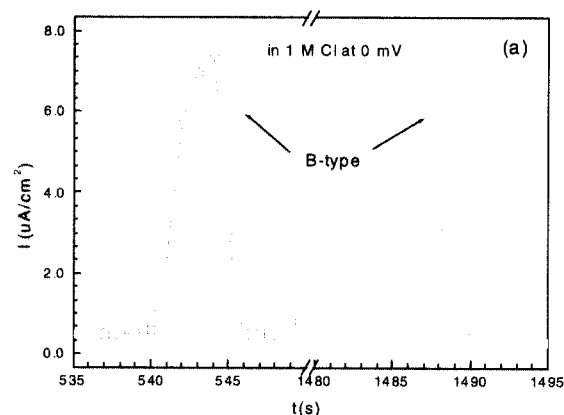


**Fig. 4.** Typical current transient generated by metastable pitting of alloy 690 in deaerated NaCl solutions at 90°C under potentiostatic conditions, (a): in 1 M Cl at 0 mV, (b) in 0.1 M Cl at 0 mV, (c) in 0.001 M Cl at 200 mV.

followed by a quick drop (we called B-type). The slow rise in current represented propagation while the quick drop of current represented the repassivation of metastable pitting.

Figure 4 illustrated these two kinds of current transients on alloy 690 in other Cl solutions under different potentiostatic conditions. We can found that propagation time

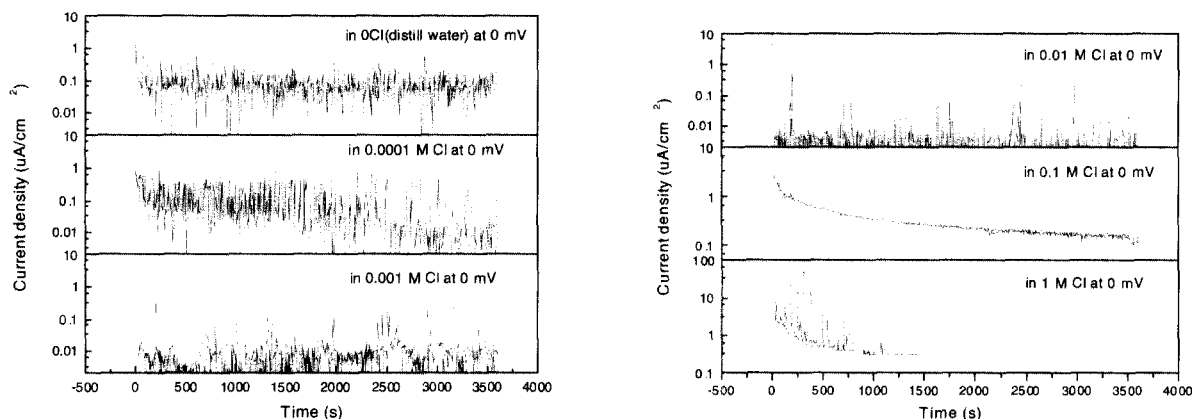


Fig. 5. Time series showing the effect of Cl<sup>-</sup> on the current spikes of metastable pitting at 0 mV in deaerated solutions at 90°C

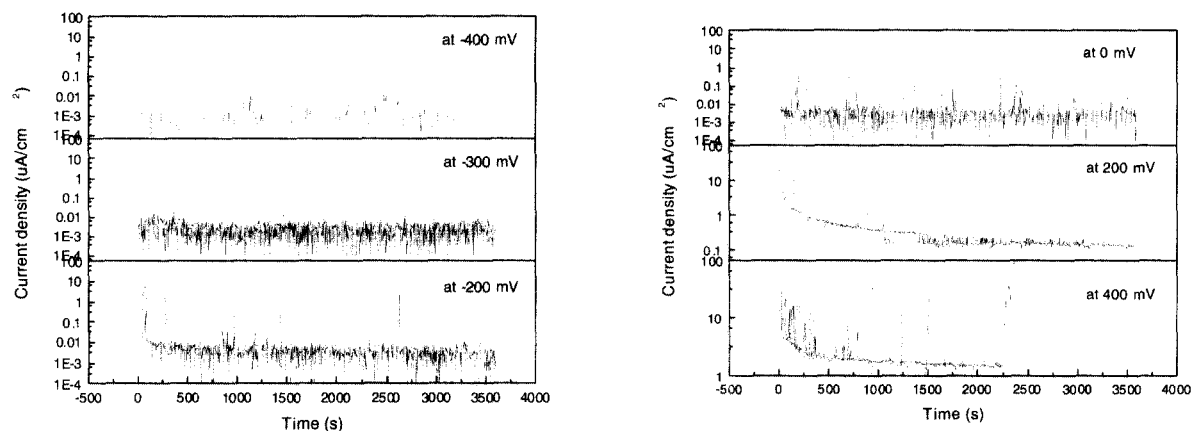


Fig. 6. Time series showing the effect of polarization potential on the current spikes of metastable pitting in deaerated 0.01 M NaCl solutions at 90°C

was varied from solution and applied potential between 1s to 5 s whereas repassivation time always lied in the range of 1 or 2 s. In other words, repassivation of alloy 690 in chloride solutions represented dependence of applied potential and concentration of chloride.

### 3.3 Influence of Cl<sup>-</sup> concentrations on metastable pitting

The influence of Cl<sup>-</sup> anion on metastable pitting was studied by using potentiostatic polarization under a constant potential in various Cl<sup>-</sup> concentration solutions. Figure 5 showed the time series at 0 mV that is below the pitting at low Cl<sup>-</sup> concentration but close to pitting potential at high concentration such as 1 M Cl solution. In distill water (free chloride ion solution), the current was characterised with high frequency fluctuations by higher background current of 0.1  $\mu\text{Acm}^{-2}$ . Similar current

fluctuation shape was obtained in 0.0001 M Cl<sup>-</sup> solution but it's worth noting that there is some differences in these two solutions. After long time polarization (about 3000s), the current in 0.0001 M Cl solution became at low level

of 0.01  $\mu\text{Acm}^{-2}$  which indicated the film was more stable than that in distill water and apparent current spikes can be distinguished from background current which was thought as metastable pitting.

In more dense Cl<sup>-</sup> solutions, the current density spikes associated with metastable pitting were observed throughout the transients and spike heights decreased with time for all solutions. Increasing with the Cl<sup>-</sup> concentration from 0.001 M to 1M, the background current density increased. In 1 M Cl solution, one of metastable pitting propagated a stable pitting.

### 3.4 Influence of applied potential on metastable pitting

The influence of potential on metastable pitting was explored by using a constant Cl<sup>-</sup> concentration of 0.01 M NaCl solution at different applied potentials from values well far below pitting potential range to that more close to the pitting potential. Figure 6 showed the current changes with time. At lower potential of -400 mV that close the flade potential, the current level is very low

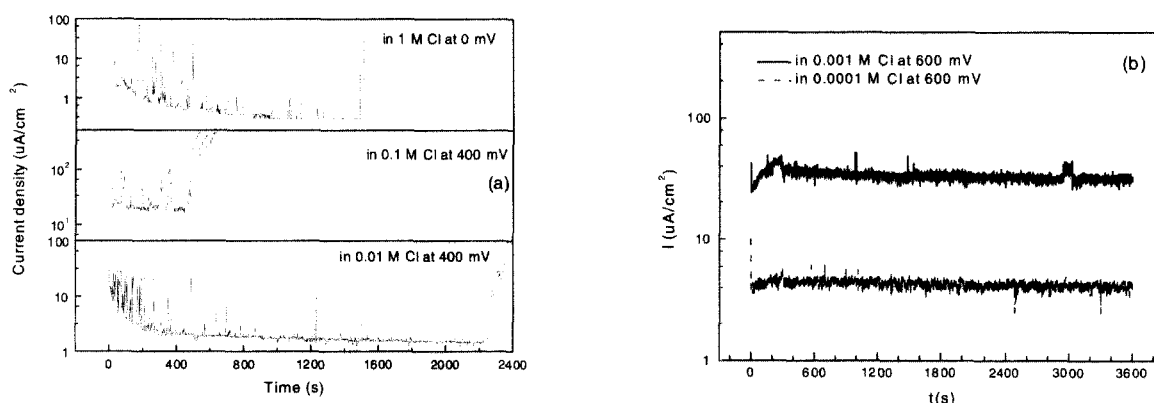


**Fig. 7.** Current responses of alloy 690 in various  $\text{Cl}^-$  solutions at  $90^\circ\text{C}$  at  $1\text{mV/s}$ , showing transition from metastable pitting to stable pitting in  $0.01\text{ M}$  to  $1\text{ M}$   $\text{Cl}^-$  solutions, transpassive dissolution in  $0.001$  and  $0.0001\text{ M}$   $\text{Cl}^-$  solutions.

(about  $10\text{nA/cm}^2$ ) and no apparent current spikes can be found. At more noble applied potential range, the current fluctuations were easily distinguished from background current and the comparison of current fluctuations indicated clearly that the number of current transients and peak current showed a general tendency to increase with the potential. At  $400\text{ mV}$ , after  $2200\text{ s}$ , stable pitting took place with high current density that propagated from a metastable pitting.

### 3.5 Transition from metastable pitting to stable pitting

Figure 7 (a) and (b) showed the current fluctuations with time of alloy 690 at more noble potential which close or over pitting potential in dense  $\text{Cl}^-$  solution ( $1$ ,  $0.1$  and  $0.01\text{ M}$   $\text{Cl}^-$  solution) or transpassive potential in dilute  $\text{Cl}^-$  solution ( $0.001$  and  $0.0001\text{ M}$   $\text{Cl}^-$ ). In dense solution, there existed a transition from metastable pitting to stable pitting on alloy 690 at different applied potentials whereas in the later solution no clear metastable pitting or stable pitting can be found even at higher potentials.

From Figure 1, we can see the metastable pitting behaviors of alloy 690 in various  $\text{Cl}^-$  solutions under potentialdynamic conditions at  $90^\circ\text{C}$ . Before the stable pitting potential, some current density spikes can be seen in all given solutions but  $0.0001\text{ M}$   $\text{Cl}^-$  solution. In  $0.1\text{ M}$  and  $0.01\text{ M}$   $\text{Cl}^-$  solutions, the height of current density can reach  $20$  to  $50\ \mu\text{A/cm}^2$ . The final pitting damage can be thought as the results of propagation from metastable pitting for alloy 690 in  $0.01$ ,  $0.1$  and  $1\text{ M}$   $\text{Cl}^-$ . In  $0.001\text{ M}$   $\text{Cl}^-$  solution, there is no transition from metastable pitting to stable pitting although some current fluctuations can be seen in the passive potential region.

## 4. Discussions

Because the metastable pitting was highly random

processes which was stochastic in nature, it's very difficult to distinguished which factor of applied potential or  $\text{Cl}^-$  concentration took main role in the metastable pitting behavior for alloy 690 in  $\text{Cl}^-$  solutions particularly in limited datas. In such cases, PSD method is a good choice to study the behavior of metastable pitting.

### 4.1 PSD analysis of metastable pitting

Power spectral density of noise was proposed to be a very powerful method to study metastable pitting. The MEM (maximum entropy method) had already been used in corrosion investigation for metastable pitting<sup>24</sup>:

In the present study, the current PSD plots of alloy 690 in various  $\text{Cl}^-$  solutions at  $0\text{ mV}$  was obtained after MEM processing with de-trending DC drift and showed in Figure 8(a). The corresponding roll-off slope changed from  $0.3$  to  $-2.5$  from  $0.0001\text{ M}$   $\text{Cl}^-$  to  $1\text{ M}$   $\text{Cl}^-$  that indicated that slope became steeper increasing with increasing of  $\text{Cl}^-$  Concentration (in Figure 8 (b)) and its PSD level indicated that same behavior with that in Figure 7(b).

Similarly, the current PSD plot and corresponding roll-off slope plot of alloy 690 in  $0.01\text{ M}$   $\text{Cl}^-$  solution at different applied potentials was showed in Figure 9 (a). The PSD level and roll-off slope increased with an increase in potential. The slope changed from  $0$  to  $-3.4$  with varying applied potential from  $-400\text{ mV}$  to  $400\text{ mV}$ . Based on the PSD analysis, we can found that frequency of metastable pitting were associated with values of PSD leveling (passive current level). In Figure 9 (a), alloy 690 in  $0.01\text{ M}$   $\text{Cl}^-$  under  $-200\text{ mV}$  and  $0\text{ mV}$  had the same PSD level and had the similar frequency of events. At the same time, PSD level had the very low values under  $-300\text{ mV}$  and  $-400\text{ mV}$  and they had the very low frequency of metastable pitting.

On the other hand, we can distinguished the corrosion type by comparing the PSD slopes. From the Figure 8(b)

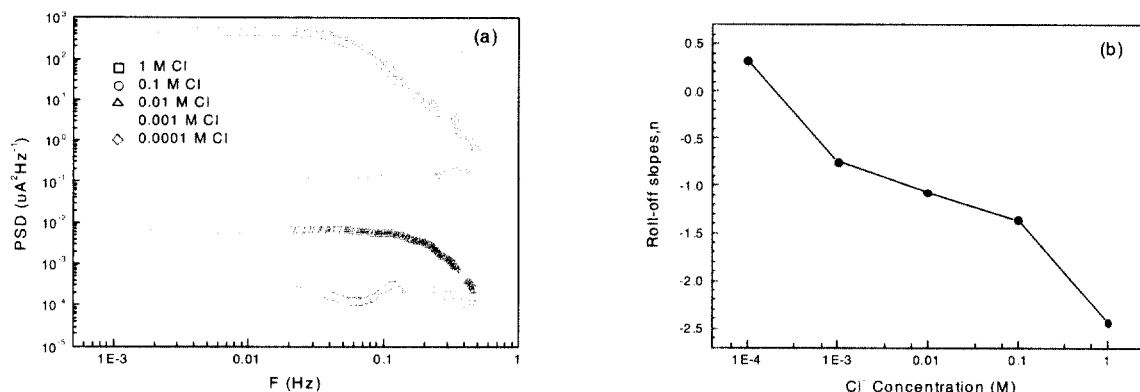


**Fig. 8.** Current PSD and roll-off slopes plots of alloy 690 in deaerated various Cl<sup>-</sup> solutions at 0 mV in deaerated solutions at 90°C, (a)PSD, de-trend DC drift, MEM plot, order 10, hanning window , data obtained from Figure 5 starting at 1024 to 2048 (in 1 M Cl, from 1 to 1024)

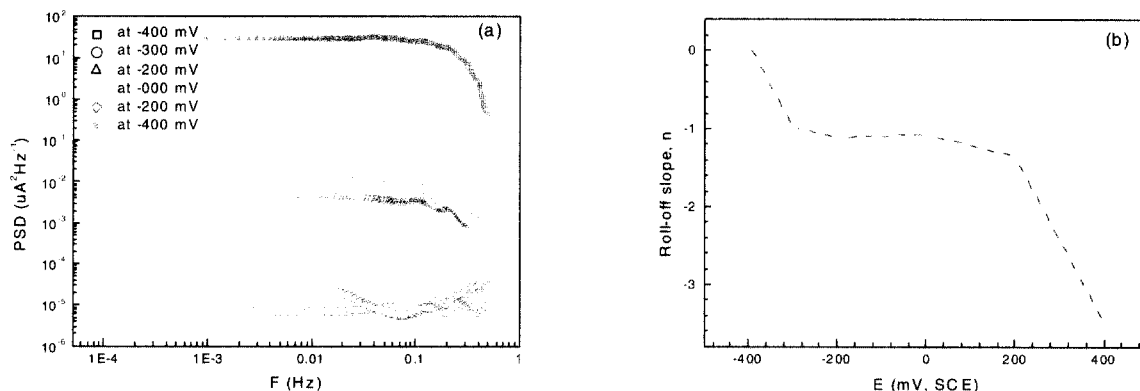


**Fig. 9.** Current PSD and roll-off slopes plots of alloy 690 in deaerated 0.01 M Cl<sup>-</sup> solutions at various polarization potentials in deaerated solutions at 90°C, (a)PSD, de-trend DC drift, MEM plot, order 10, hanning window, data obtained from Figure 6 starting at 1024 to 2048, (b) roll-off slopes

and Figure.9 (b), we can found that the values of roll-off slope of -1 was corresponded to metastable pitting whereas that large value which above 0 mV for no metastable pitting (for -400mV in 0.01M Cl or 0 mV in 0.0001MCl, just some current fluctuations for film formation and dissolution) or negative values which smaller than -2.5 for pitting corrosion (eg. 1M Cl in 0 mV or 400 mV in 0.01 M Cl). This was similar with the result of Luo<sup>15)</sup> on carbon steel.

From above analysis, we can found that PSD leveling and roll-off slope can easily distinguished the different characteristic on alloy 690 in different solutions or different applied potentials and it's a powerful tool to perform the research on metastable pitting.

#### 4.2 metastable pitting, alloy 690, chloride solution, power spectral density.

D.E Williams et. al, proposed a model to explain the

passivity breakdown and pitting corrosion of binary alloys and this model can be used in this study.<sup>25)</sup> In their model, they thought pitting corrosion of stainless steels could be explained by assuming that it is controlled by selective dissolution of iron. Oxidation of surface chromium atoms to form Cr-O-Cr linkages then created a passive state in which the entire surface was covered with such a layer if chromium content is above a certain threshold. Our work [26] indicated that enrichment of Cr took place in the outmost layer of passive film on 690 in buffer solutions. So, in the present study, we can get that pitting corrosion is caused mainly by the dissolution of Fe or Ni whereas Cr didn't took place pitting in 1M Cl solution.

In potentiostatic conditions, in the first time range about 1000s, there existed larger frequency and higher heights current transients that were ascribed as dissolution of clusters of iron or nickel atoms in the surface of alloy. The frequency of the current spikes decreased with time

owing to elimination of these clusters. Passing the long time, the passive current is nearly constant and frequency varied little with time that was consisted with the experimental results.

At less aggressive environment, eg. Dilute Cl solution (0.0001MCl) or less noble applied potential (-400 mV or -300 mV in 0.01MCl), the rate of dissolution of Ni and Fe is limited, so, susceptibility of metastable pitting is low. Increasing with the polarization condition, passive current increased that increased the dissolution probability of chromium, which determined the rate of uncovering the iron and nickel clusters and increased susceptibility of metastable pitting. In more aggressive conditions such high applied potential (400 mV in 0.01MCl) or dense Cl solutions (1MCl), not only Ni or Fe but also Cr had large dissolution rate that can cause more rapid dissolution of uncovering of the Fe and Ni cluster and caused pitting corrosion. Chloride anion, as the most common aggressive ion, played main roles in dissolution of Fe, Ni and Cr and alloy 690 which was constituted by these elements. As mentioned before, there existed a critical concentration to cause pitting corrosion of alloy 690 which was easily understand that accumulation of such anions into the cluster sites can determine the rate of dissolution of these clusters.

## 5. Conclusions

1) There existed metastable pitting prior to pitting corrosion of alloy 690 in Cl solutions and pitting corrosion was developed from metastable pitting.

2) There existed a critical concentration of Cl of 0.01M above that alloy 690 can take place the pitting corrosion and there is a distribution of pitting potentials.

3) Metastable pitting spikes were characterized by a slow rise in current followed by a quick drop.

4) Repassivation of metastable pitting of alloy 690 in given conditions is independent of applied potentials and Cl concentrations.

5) PSD by MEM is a useful tool to study of metastable pitting and PSD leveling indicated susceptibility of metastable pitting

6) Corrosion type can be distinguished by the PSD slopes of that 0 represent film dissolution, -1 represented metastable pitting and -2.5 represented pitting corrosion.

7) A model proposed by D.E. Williams of can be used explain the mechanism of metastable pitting of alloy 690 in given conditions.

## References

1. D. R. Diercks, W. J. Shack, J. Muscara, *Nuclear Engineering and Design* **194**, 19 (1999).
2. J. T. Ho and G. P. Yu, *Corrosion*, **48**(2), 147 (1992).
3. W. T. Tsai T. F. Wu, *Journal of Nuclear Materials*, **277**, 169 (2000)
4. M. Y. Chang and F. P. Yu, *Journal of Nuclear Materials*, **202**, 145 (1993).
5. L. J. Yang, *Materials Chemistry and Physics* **49**, 50 (1997).
6. S. S. Hsu, S. C. Tsai, J. J. Kai and C. H. Tsai, *Journal of Nuclear Materials* **184**, 97 (1991).
7. A. Legat, V. Dolecek, *J. Electrochem. Soc.* **42**, 1851 (1995).
8. C. Gabrielli, F. Huet, M. Keddam et al., *Corrosion* **46**, 266 (1990).
9. L. F. Garfias-Mesias, J. M. Sykes, *Corrosion Science* **41**, 959 (1999).
10. P. C. Pistorius and G. T. Burstein, *Phil. Trans. R. Soc. Lond. A*, **341**, 531 (1992).
11. P. C. Searson, J. L. Dawson, *J. Electrochem. Soc.*, **135**, 885 (1988).
12. B. Wu, J. R. Scully and J. L. Hudson, *J. Electrochem. Soc.*, **144**, 1614 (1997).
13. S. T. Pride, J. R. Scully and J. L. Hudson, *J. Electrochem. Soc.* **141**, 3028 (1994).
14. Y. F. Cheng, M. Wilmott and J. L. Luo, *Applied Surface Science* **152**, 161 (1999).
15. Y. F. Cheng, J. L. Luo, *J. Electrochem. Soc.* **146**, 161 (1999).
16. Y. F. Cheng, J. L. Luo, *Electrochimica Acta*, **44**, 2947 (1999).
17. G. S. Frankel, *J. Electrochem. Soc.*, **145**, 2186 (1998).
18. P. E. Doherty, M. J. Psaila-Dombrowski, S. L. Harper et al, in ASTM STP 1277, Jeffery S. Kearns et al. Eds., pp.288-304 (1996).
19. G. M. W. Mann and R. Castle, EPRI Topical Rep., NP-3050, (1983).
20. Z. Fang and R.W. Staehle, *Corrosion*, **55**, 355 (1999).
21. J. J. Kai, G. P. Yu, C. H. Tsai, et al., *Metallurgical Transactions A*, **20A**, 2057 (1989)
22. H. B. Park, Y. H. Kim, B. W. Lee, *Journal of Nuclear Materials* **231**, 204 (1996).
23. J. J. Kai, C. H. Tsai, T. A. Huang *Metallurgical Transactions*, **20A**, 1077 (1989).
24. U. Bertocci, J. Frydman, C. Gabrielli, *J. Electrochem. Soc.* **145**, 2780 (1998).
25. D. E. Williams, R. C. Newman, Q. Song *Nature*, **350**, 216 (1991).
26. Z. J. Bai, H. S. Kwon, "Electronic structure of passive films on alloy 600 and alloy 690 in buffer solution", prepared.